COOLANT PASSAGE HEAT TRANSFER WITH ROTATION*

T.J. Hajek
Pratt & Whitney Division
United Technologies Corporation
East Hartford, Connecticut

and

J.H. Wagner and B.V. Johnson
United Technologies Research Center
East Hartford, Connecticut

In current and advanced gas turbine engines, increased speeds, pressures and temperatures are used to reduce specific fuel consumption and increase thrust/weight ratios. Hence, the turbine airfoils are subjected to increased heat loads, escalating the cooling requirements to satisfy life goals. The efficient use of cooling air requires that the details of local geometry and flow conditions be adequately modeled to predict local heat loads and the corresponding heat transfer coefficients.

Improved turbine airfoil local temperature and hence, life predictions can be realized by accurately accounting for the effects of rotation on internal cooling. Although the effects of rotation, which give rise to Coriolis and buoyancy forces can be large, they are currently not adequately included in the heat transfer designs of blades. Experimental data is particularly needed for the higher Rayleigh and Reynolds number conditions that are characteristic of turbine airfoil cooling passages. This data is crucial for development of design correlations and for the verification of computer codes. Accurate prediction of local heat transfer coefficients will enable the designer to optimize cooling configurations and to minimize both metal temperature levels and thermal gradients. Consequently, blade life and engine efficiency can be significantly improved.

OBJECTIVE

The objective of this 36-month experimental and analytical program is to develop a heat transfer and pressure drop data base, computational fluid dynamic techniques and heat transfer correlations for rotating multipass coolant passages, with and without flow turbulators. The experimental effort is focused on the simulation of configurations and conditions expected in the blades of advanced aircraft high pressure turbines. With the use of this data base, the effects of Coriolis and buoyancy forces on the coolant side flow can be included in the design of turbine blades.

EXPERIMENTAL MODEL

The heat transfer model features a four pass serpentine arrangement, designed to reflect the coolant passages within a gas turbine blade. For the experiments, the model was fitted with smooth walls on all four walls or with skewed turbulators on two walls, as indicated in figure 1.

* NASA Contract NAS3-23691

Figure 2 shows a schematic diagram of the model with the instrumentation and wall sections indicated. Heat transfer coefficients are obtained for each wall section element. These wall elements, numbered 1 to 64, consists of a copper block backed with a thin film electrical resistance type heater and instrumented with two thermocouples. The copper wall sections are 10.7 mm. x 49.3 mm. (0.42 in. x 1.94 in.). Each section is thermally isolated from the adjoining section by a 1.5 mm. (0.060 in.) thick divider strip of low thermal conductivity G-11 composite material. The straight radial passages have a square cross section, 12.7 mm. x 12.7 mm. (0.5 in. x 0.5 in.).

DATA ACQUISITION AND REDUCTION

Sixty (60) experiments have been conducted to isolate the effects of rotation rate, flow rate, coolant-to-wall temperature variations, radial location and passage angle on heat transfer from the smooth and skewed trip models. These heat transfer experiments have been conducted with all the wall segments at a constant temperature. The data consists of measurements of thermocouple emf and heater power for each heated element. Engineering results are obtained with an analysis code and then printed in tabular form.

An energy balance is performed to determine the heat transfer characteristics for the model at each experimental condition. The energy convected to the coolant is determined by subtracting the energy lost through the power leads and the energy lost through the conduction from the backside of each element. The bulk-mean coolant temperature for a particular location in the passage is determined by summing the energy contributions from each element. The temperature increase from the inlet location is then calculated using simple thermodynamic relationships. The heat transfer coefficient is calculated with the local coolant and wall temperatures and the local net energy (or heat) flux.

A more complete description of the acquisition/analysis procedure is provided in the 1986 HOST report.

RESULTS

The heat transfer experiments with the smooth wall model and the 45-deg skewed trip rough wall model were completed prior to the previous HOST conference. Detailed analysis of results has continued throughout the past 12 months. The heat transfer characteristics of the flows in the first outward flow leg and the inward flowing leg are compared in this report. The effects of model orientation are also discussed.

The variations of heat transfer ratio, Nu/Nu_∞, from the leading and trailing surfaces with rotation parameter, $(\Omega d/V)$, are presented for the first and second leg in figure 3. The ΔT noted on the figure refers to the temperature difference between the coolant (at the inlet to the first leg) and the walls. The local ΔT's in the second leg of the rough wall model are 40 to 50 percent of the inlet ΔT due to the increase in fluid bulk temperature in the two legs and the first turn. Note that the heat transfer varies with both the rotation rate and the inlet-air-temperature to wall-temperature difference, ΔT. For all the data shown, the heat

transfer increases or remains constant with increasing ΔT. The magnitude of the increase, ΔNu, can be as large or larger for the rough wall model as it is for the smooth wall model (trailing surfaces for all segments shown). However, the percent changes are generally smaller for the rough wall model because the heat transfer level is higher. Note also that large increases and decreases in the heat transfer occurred due to variations in the rotation parameter. The most dramatic decrease with increasing rotation occurred for the rough walls on the leading surface of the first leg (with outward flow). The third principal feature of these results is that the effects of temperature difference generally increase at larger values of the rotation parameter, $\Omega d/V$. For both the smooth wall model and the rough wall model, the heat transfer was independent of ΔT at zero rotation. This result at zero rotation was consistent with previous studies. In view of the three previous observations, it was concluded that the rotation heat transfer results could not be correlated with only the rotation parameter.

The variation of the heat transfer ratio with the buoyancy parameter, $(\Delta\rho/\rho)(\Omega H/V)(\Omega d/V)$, is shown in figures 4a-f. The solid lines in the figure connect the heat transfer results from the experiments where the temperature difference between the inlet coolant and the wall were the largest. The dotted lines connect the results for experiments with similar rotation parameters but different inlet air to wall temperature differences, ΔT. In general, the heat transfer for any location on the high pressure side of the coolant passages is well correlated by the buoyancy parameter. The high pressure sides are the trailing side for flow outward and the leading side for flow inward. The secondary flow patterns generated by Coriolis forces are characterized by a redirection of the flow from the core of the passage toward the high pressure side of the passage. Note that the heat transfer ratio on the high pressure side of the outward flowing leg for both models does not change appreciably with streamwise location at higher values of the buoyancy parameter. The heat transfer from the high pressure side of the inward flowing leg decreases monotonically with increasing streamwise location.

In the second leg (figs. 4d-f), the flow direction and the buoyancy force are in the same direction. In this passage leg, the heat transfer is substantially decreased compared to that from the first leg. This decrease may be due to the change in the turbulent structure near the wall when the flow direction changes from the opposing-the-buoyance-force direction to the coinciding-with-the-buoyancy force direction.

The buoyancy parameter does not correlate the heat transfer results from the low pressure side of the passage as well as those from the high pressure side. For the first segment (fig. 4a), the heat transfer ratio on the low pressure side is a function of both rotation rate (different symbols) and the temperature difference (different flags). Note that the relative variation of heat transfer ratio with ΔT (at fixed rotation number) are greater for the smooth wall than the rough wall. The heat transfer ratios for the leading surface appear to have a maximum value for each rotation number. The locus of the maximum heat transfer ratios for each rotation number appears to be a function of the buoyancy parameter. The heat transfer ratio distributions from the skewed trip leading surface for fixed rotation numbers have shapes similar to the heat transfer ratio distributions for the smooth leading surface. At the downstream segment in

the first leg (fig. 4C), the heat transfer ratio for the smooth wall becomes well correlated by the buoyancy parameter. The correlation of the leading surface smooth wall results at the end of the first leg suggests that correlation of the results may be related to the hydrodynamic or thermal development of the flow. Heat transfer results from the inward flowing leg show similar variations of heat transfer ratio with temperature difference and rotation parameter. The decrease in the temperature dependence on the heat transfer ratios between the first and second legs is attributed in part to the decrease in the local ΔT as the flow.

Comparison of the heat transfer ratios from the smooth and skewed trip models show that, at zero rotation rate (zero buoyancy parameter), the heat transfer ratio from the smooth wall and skewed trip models is determined by the geometry of the coolant passages (i.e. smooth surfaces produce low heat transfer coefficients and surfaces with skewed trips produce high heat transfer coefficients). For large buoyancy parameters, the leading and trailing surface heat transfer distributions from the end of the first leg for both the smooth wall and skewed trip models asymptotically approach their respective levels. Half of the difference in the heat transfer ratio between the smooth wall and the skewed trip models for large buoyancy parameters on the trailing surface of the first leg can be attributed to the ratio of the actual surface area compared to the projected area used in the calculation of the heat transfer coefficients. In the outward flowing leg at a large value of L/d, the rotational buoyancy dominates the heat transfer more than the surface roughness at large (i.e. greater than 0.6) values of the buoyancy parameter.

Effect of Model Orientation

Heat transfer experiments with rotation were completed with both the smooth and skewed trip model oriented at α=45 degrees from the normal position. The model was rotated 45 degrees about the radial centerline such that the inlet of the model was trailing the centerline of the model. This orientation was selected to model the coolant passages in a turbine blade with a trailing edge root feed. The heat transfer ratios around the perimeter of the coolant passage for each streamwise location in the first passage are shown in figures 5 and 6. The model orientation and rotation direction are noted on each figure. Results from the smooth wall model have been connected with a continuous line because the model is symmetrical (fig. 5). However, the skewed trip results (fig. 6) are connected to show only the changes in heat transfer on each of the four walls from one orientation to the next. The heat transfer results for the smooth wall model show a symmetrical pattern around the perimeter of the passage. At α=45 deg, the two leading surfaces have approximately the same heat transfer ratio as the one leading surface for α=0. Likewise, at α=45 deg, the two trailing surfaces have approximately the same heat transfer ratios as the trailing surface for α=0 deg.

The heat transfer results for the skewed trip model (fig. 6) indicate an asymmetry in the heat transfer around the perimeter of the coolant passages due to the presence of the skewed trips. For this reason, the results are not connected around the perimeter as they were for the smooth wall results. Note that the heat transfer ratio is significantly larger for the sidewall surface on the bottom of each plot than that for the side wall surface on the top of each plot for segments B, C and D. These

"bottom" sidewall locations are located on the "downstream" end of the trips (see fig. 2, surfaces 2-4). The heat transfer is increased on the "downstream" surfaces due to the redirection of the main core flow along the skewed trip to these surfaces. The heat transfer ratio from the last "downstream" sidewall segment is the largest because of the development of trip generated secondary flow. In general, the heat transfer from the first leg of the skewed wall model was affected less by the change in orientation from $\alpha = 0$ to 45 deg than the heat transfer from the smooth wall model.

Streamwise location of test sections identified by A to R.
All four test section surfaces for streamwise locations A through R are heated.

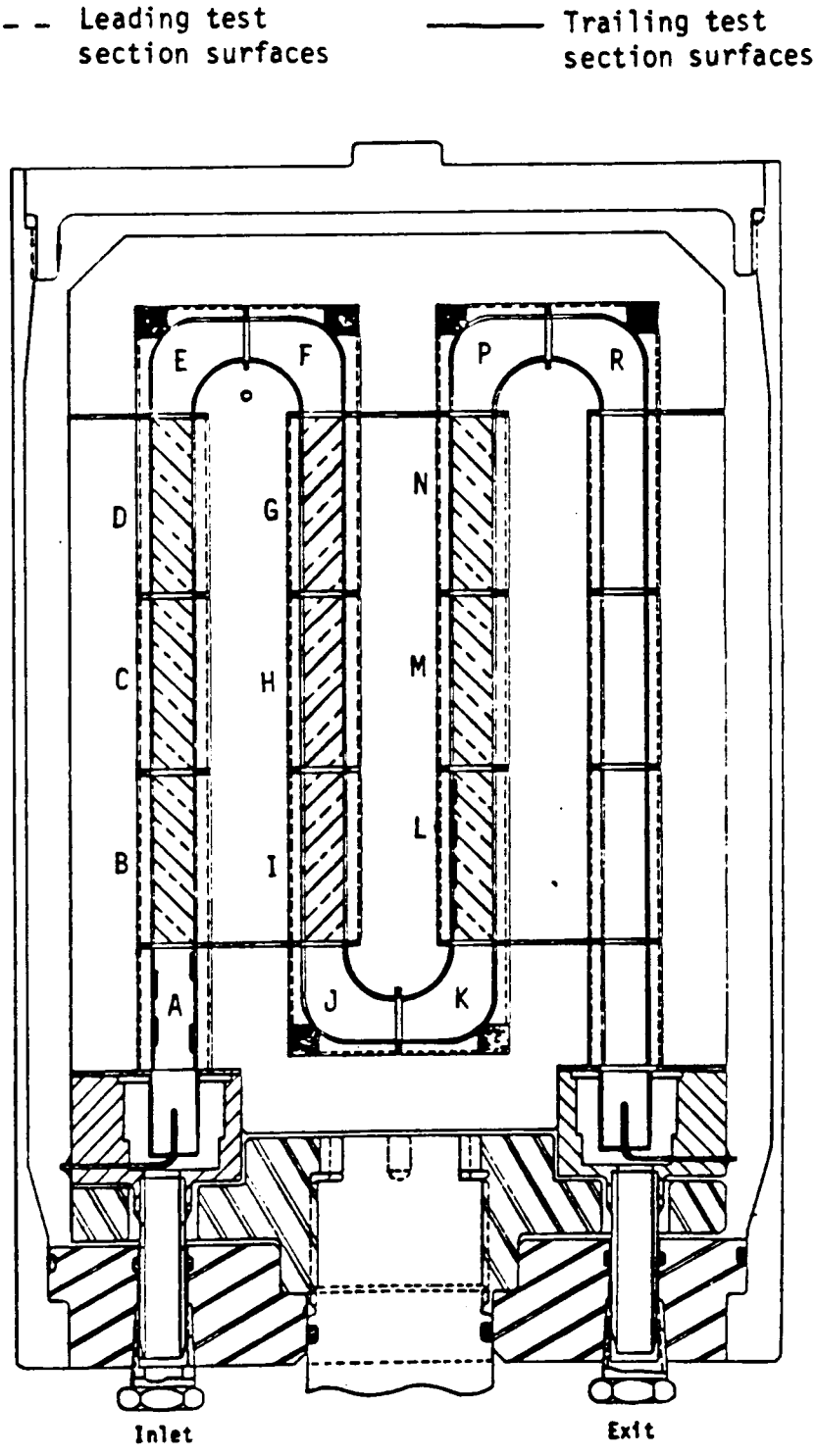

Figure 1 Cross Sectional View of Coolant Passage Heat Transfer Model Assembly With Skewed Trip Rough Walls

TEST SECTION ELEMENT IDENTIFICATION
SURFACES 1-32 ARE ON SIDE WALLS PERPENDICULAR TO VIEW SHOWN
SURFACES 33-48 ARE ON "+Ω" LEADING PLANE
SURFACES (49)-(64) ARE ON "+Ω" TRAILING PLANE
PRESSURE MEASUREMENT LOCATIONS [1] – [16]

NOTE EACH TEST SECTION SURFACE IS INSTRUMENTED WITH TWO THERMOCOUPLES

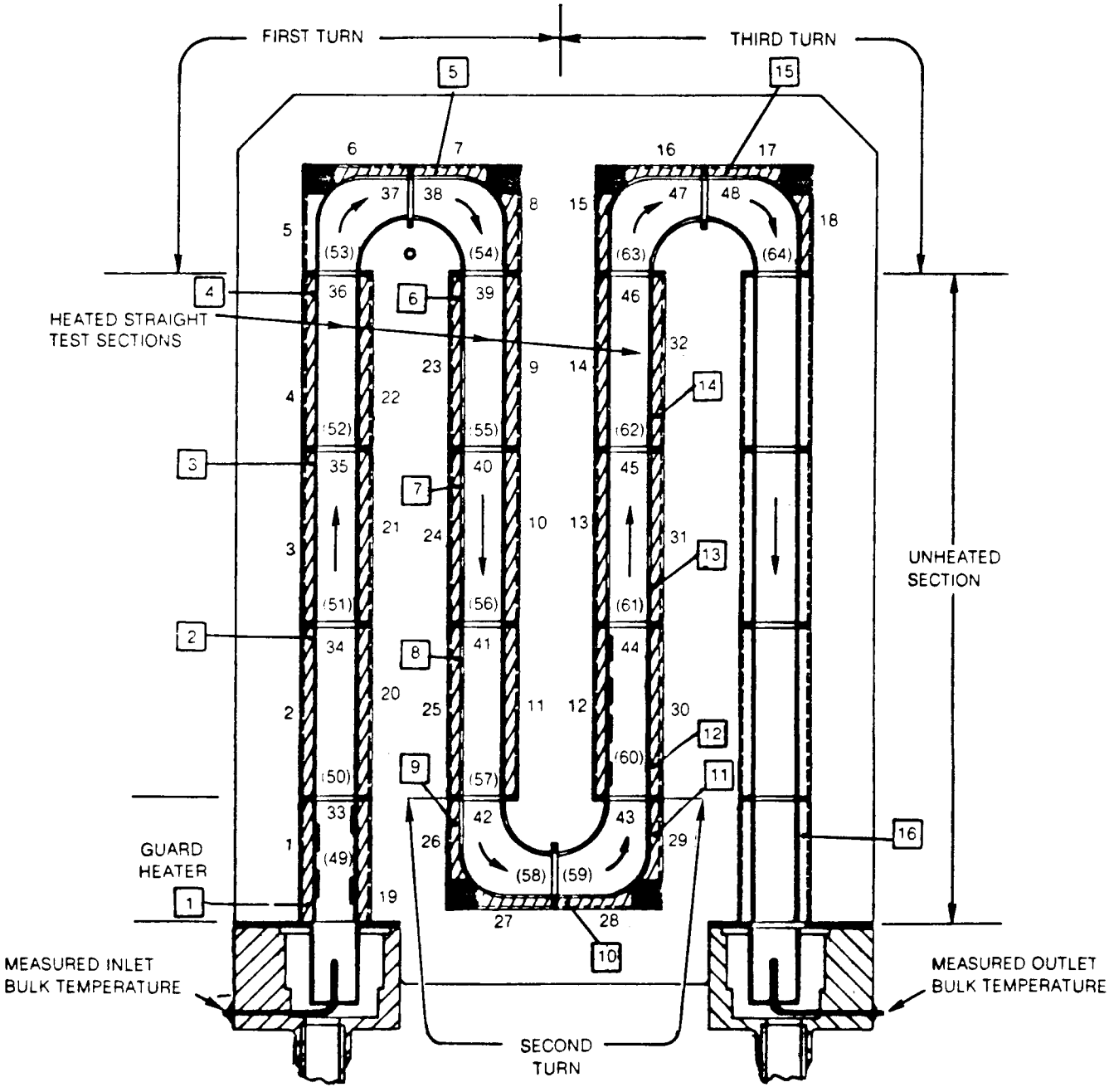

Figure 2 Instrumentation Plan for Coolant Passage Heat Transfer Model

Re = 25,000
Open Symbols - Smooth Wall
Solid Symbols - Rough Wall

	Symbol Flags
$\Delta T = 40^{\circ}F$	
$\Delta T = 80^{\circ}F$	
$\Delta T = 120^{\circ}F$	
$\Delta T = 160^{\circ}F$	

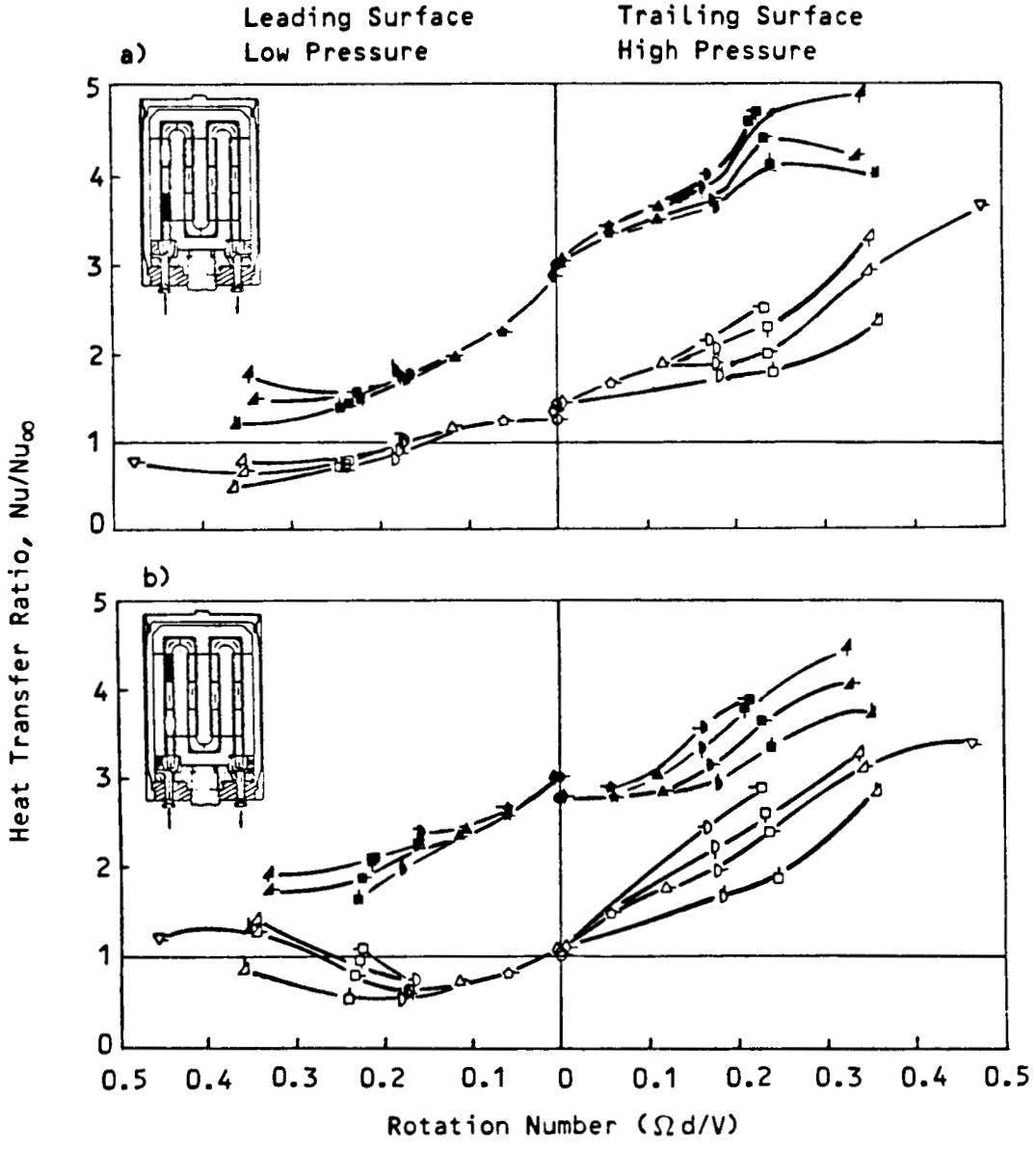

Figure 3 Effect of Rotation Number on Heat Transfer Ratio for Smooth Wall and Rough Wall Models

Re = 25,000
Open Symbols - Smooth Wall
Solid Symbols - Rough Wall

	Symbol Flags
$\Delta T = 40^{\circ}F$	○
$\Delta T = 80^{\circ}F$	○
$\Delta T = 120^{\circ}F$	○
$\Delta T = 160^{\circ}F$	○

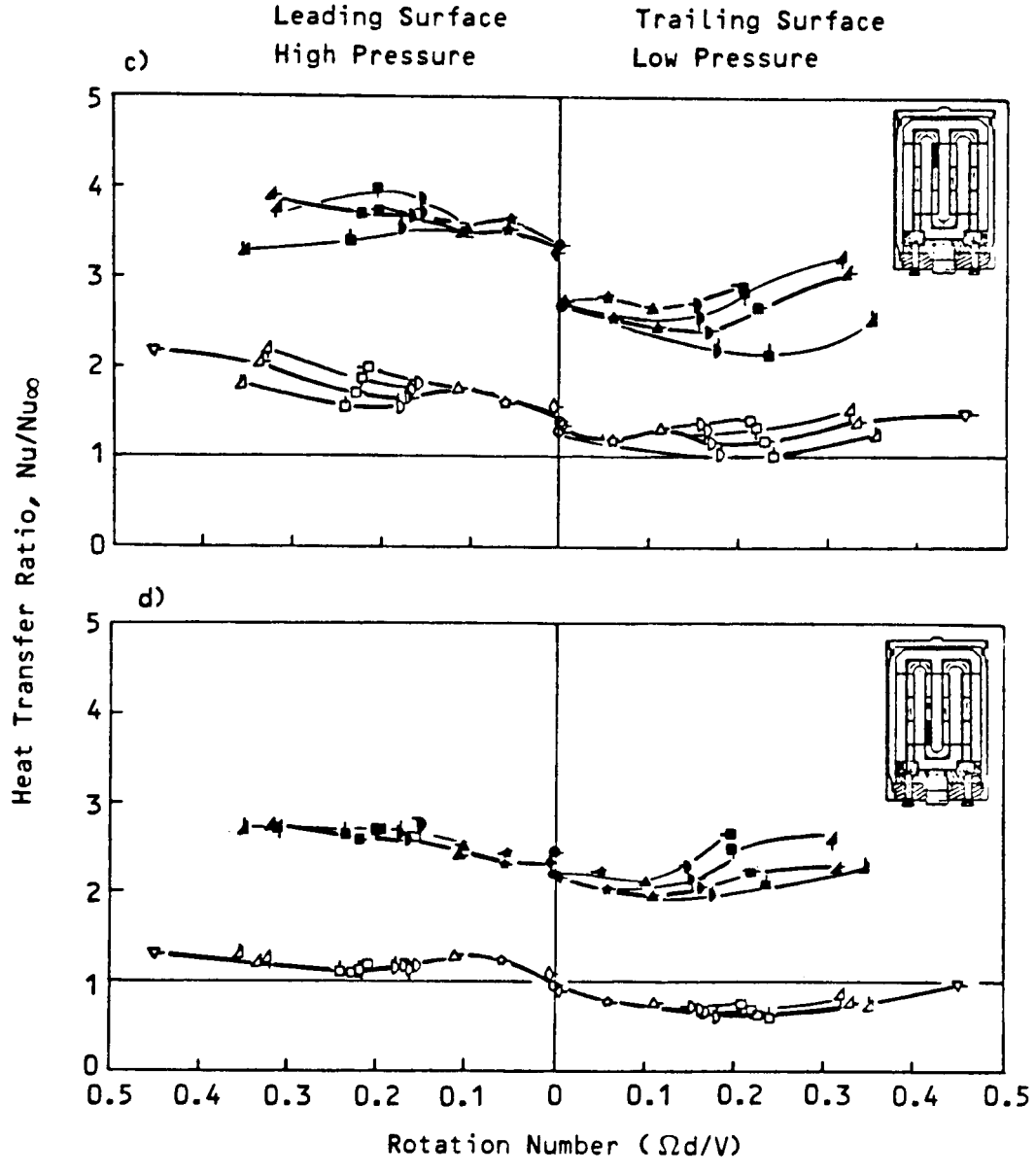

Figure 3 (Concluded) Effect of Rotation Number on Heat Transfer Ratio for Smooth Wall and Rough Wall Models

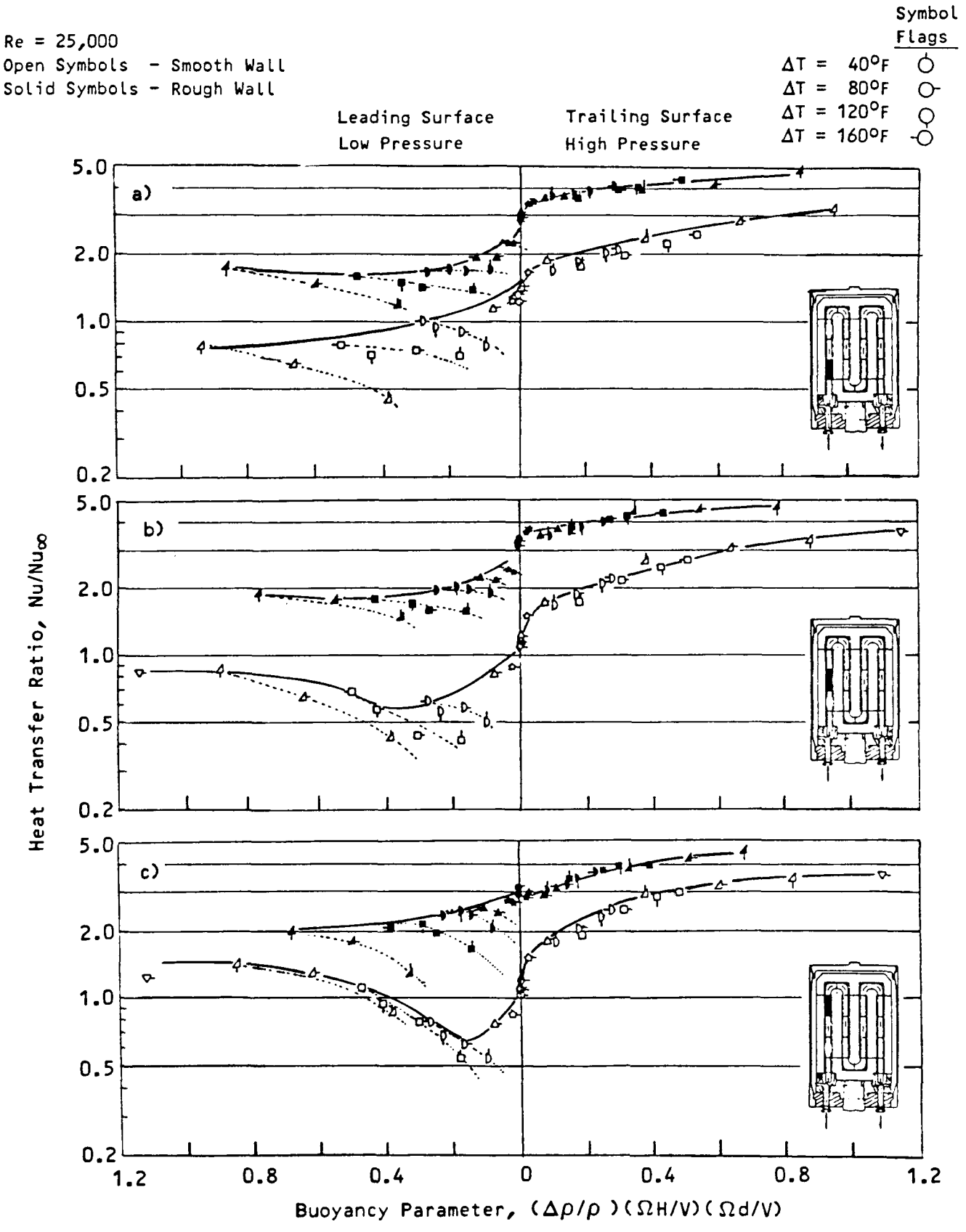

Figure 4 Effect of Buoyancy Parameter on Heat Transfer Ratio for Smooth Wall and Rough Wall Models

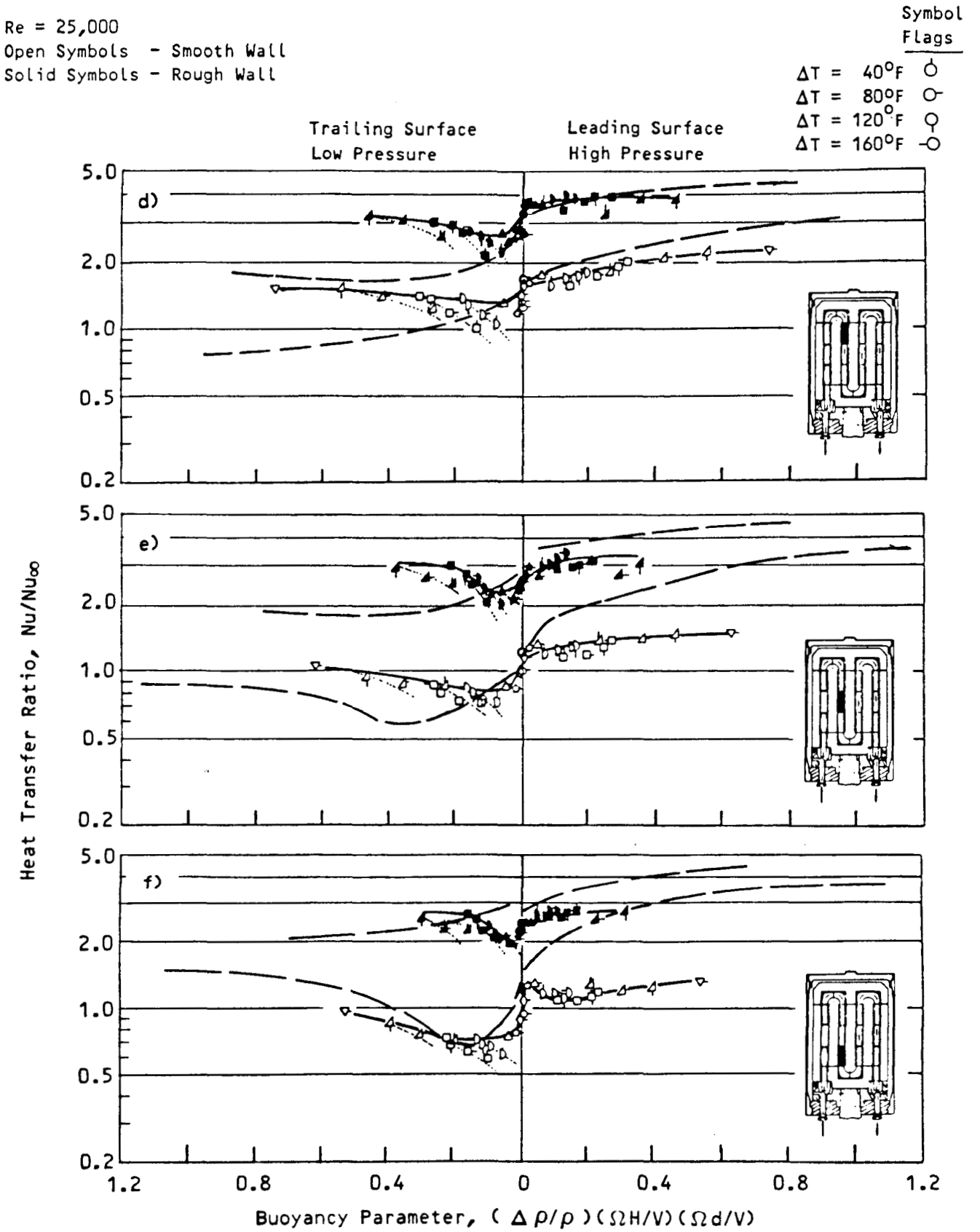

Figure 4 (Concluded) Effect of Buoyancy Parameter on Heat Transfer Ratio for Smooth Wall and Rough Wall Models

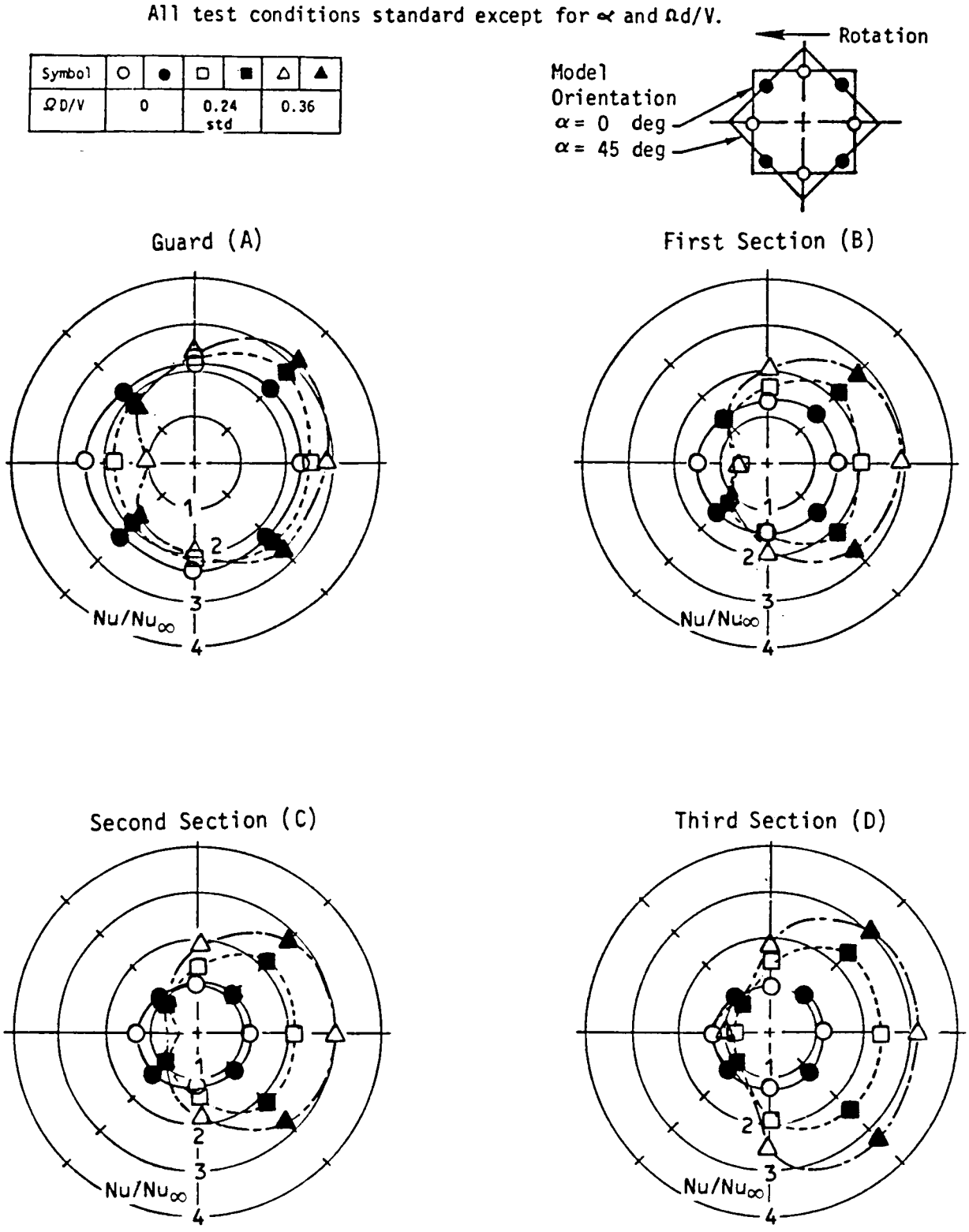

Figure 5 Variation of Heat Transfer Ratio Around Test Sections With Streamwise Locations, Rotation Number and Model Orientation for First Leg of Smooth Wall Model

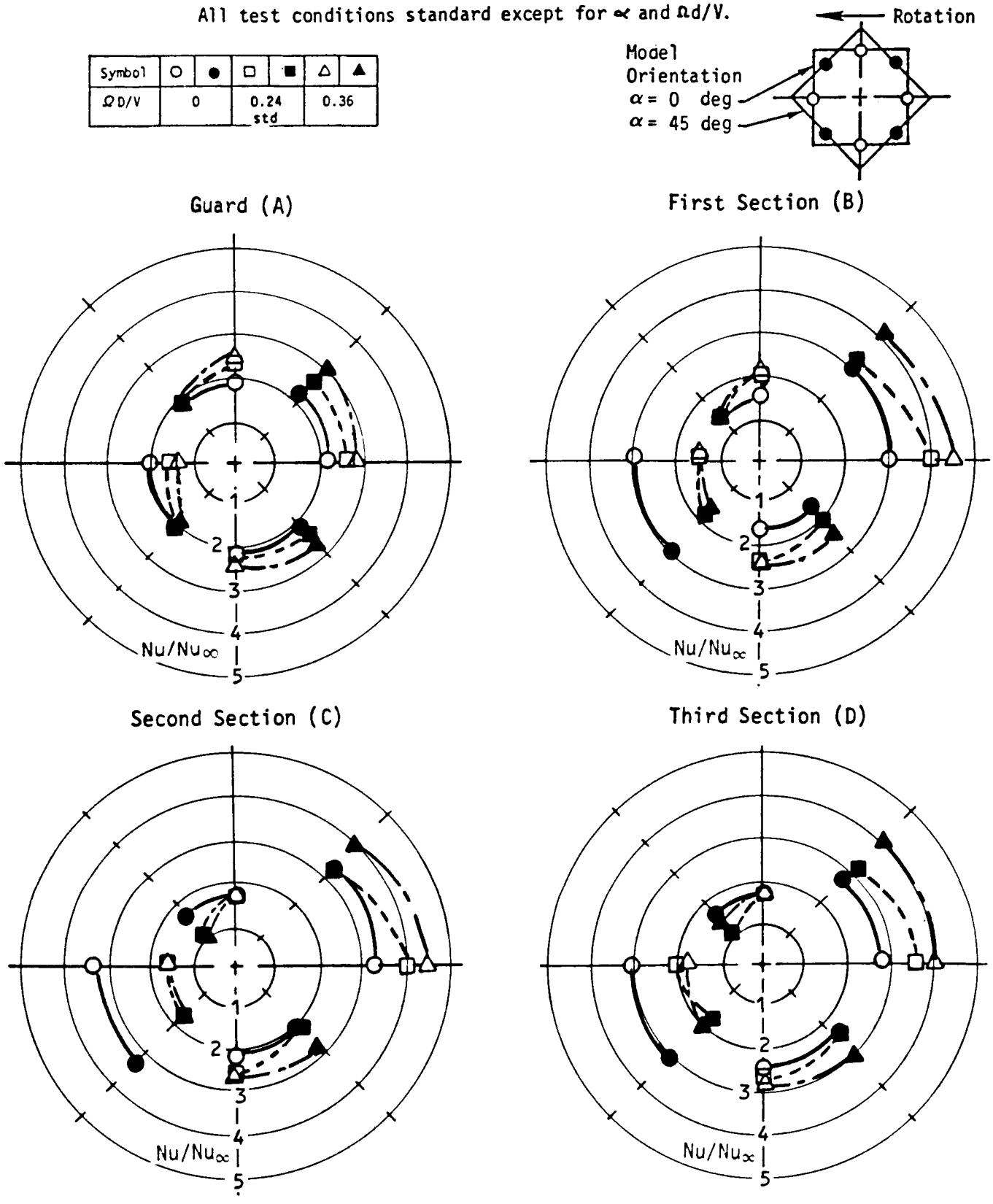

Figure 6 Variation of Heat Transfer Ratio Around Test Section With Streamwise locations, Rotation Number and Model Orientation for First Leg of Rough Wall Model